NEXT GENERATION ANODES FOR LITHIUM-ION BATTERIES: MATERIALS ADVANCEMENTS

Silicon Deep Dive

ZHENGCHENG (JOHN) ZHANG

2017 U.S. DOE HYDROGEN and FUEL CELLS PROGRAM and VEHICLE TECHNOLOGIES OFFICE ANNUAL MERIT REVIEW AND PEER EVALUATION MEETING
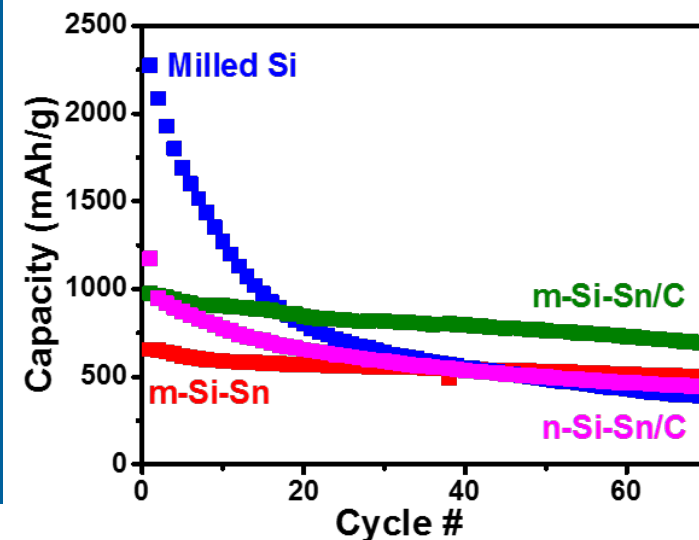
Project ID ES335

OVERVIEW

Timeline

- Start: October 1, 2015
  - Reset: October 1, 2016
- End: September 30, 2019
- Percent Complete: 40%

Budget

- Total project funding:
  - FY 17 - $3600K
- ES261 and ES335

Barriers

- Development of PHEV and EV batteries that meet or exceed DOE and USABC goals
 - Cost, Performance, and Safety

Partners

- Sandia National Laboratories
- Oak Ridge National Laboratory
- National Renewable Energy Laboratory
- Lawrence Berkeley National Laboratory
- Argonne National Laboratory

RELEVANCE

Battery Performance and Cost (BatPaC) Model Utilized to Establish Relevance by Connecting Pack to Anode Targets

- Pack level benefits reach diminishing returns after **1000 mAh/cm³** for both cost and energy density
  - mAh/cm³ [electrode basis] = $\rho \cdot \varepsilon \cdot Q$ [$g/cm^3_{act} \cdot cm^3_{act}/cm^3_{elect} \cdot mAh/g$]
- Silicon with <75 wt% graphite can achieve target
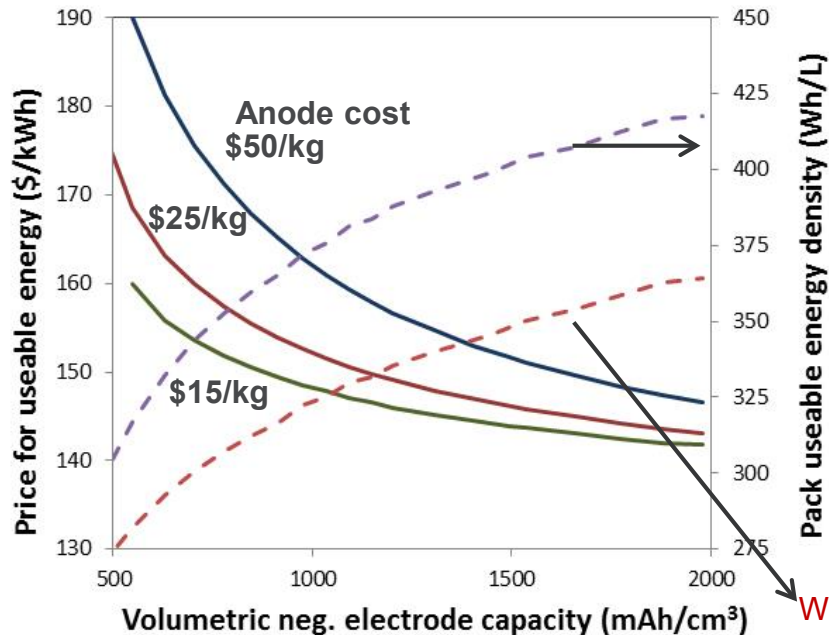
45 kWh$_{use}$, 90 kW 360 V
$20/kg 200 mAh/g NMC cathode

Wh/L including foam between cells 2x volume expansion
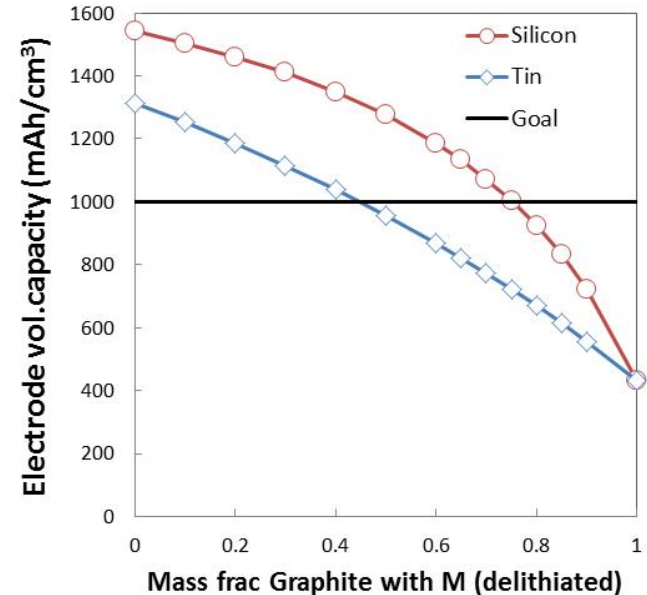
Electrode volumetric capacity uses lithiated basis Li$_{4.4}$Si or Li$_{4.4}$Sn and maximum active material volume fraction of 65%

APPROACH

❑ A multiple technical approach was employed to tackle the issues associated with the Si anode in this Deep-Dive program (Ref. ES261).

    ✓ Alternative high-energy metals: $Me_xSi_{0.66}Sn_{0.34}$ (Me: Cu, Ni, Fe, Mn).
    ✓ Interfacial modifications by Atomic or Molecular Layer Deposition (ALD or MLD) and *in-situ* formation of robust SEI by functional electrolyte/additive.
    ✓ Functional polymer binders for improved adhesion and performance
    ✓ Lithium inventory to offset the large irreversible capacity of Si anode.

❑ Resources and scientific intelligence are shared within this consortium to promote the discovery of new materials and new technologies and to facilitate the successful application of high capacity Si anode in the next generation high energy high power lithium-ion battery for electric vehicle application.

❑ New materials will be scaled-up with the support of MERF and incorporated into the baseline Silicon-based materials, electrodes and cells (SiBMECs) with support of CAMP and BMF.
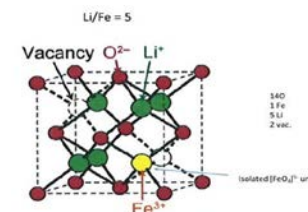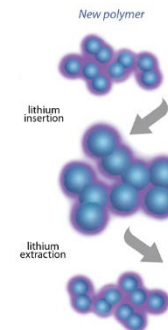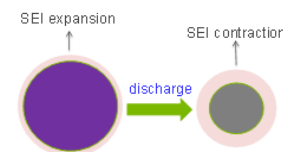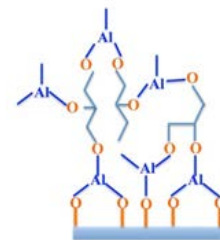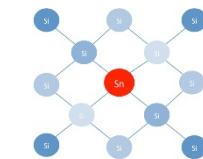
MILESTONES AND ACTIVITIES

- **The program has more than twenty-five milestones related to the broad range of interactive activities listed below.**
- **Generally, milestones are either completed or on schedule except for aqueous-based silicon electrode process development, whose challenges are described in more detail in the technical section.**

- Extensive electrochemical and analytical diagnostic studies.

- Facilities supporting program through a wide range of studies.
  - Battery Abuse Testing Laboratory (BATLab); Battery Manufacturing Facility (BMF); Cell Analysis, Modeling, and Prototyping (CAMP); Materials Engineering Research Facility (MERF); Post-Test Facility (PTF)

- Development and testing of coatings and additives designed to modify and stabilize the interface.

- Develop and analyze polymer binders designed to accommodate volume changes, increase conductivity, and improve adherence.

- Active material development.
  - Explore lithium inventory strategies.
  - Study alternative high-energy metals.

For reviewers, a detailed list of the milestones was included in the reviewers only slides in ES261.

Sandia National Laboratories

OAK RIDGE National Laboratory

NREL NATIONAL RENEWABLE ENERGY LABORATORY

BERKELEY LAB

Argonne NATIONAL LABORATORY

1. Silicon-Tin (Si-Sn) Alloy Materials

- Alloying combination of active elements often results in electrochemical behavior, which is unlike the parent elements.
- Addition of active metals to Si can have profound effects on its electrochemical performance.
- When Si is present in nanosized regions within a matrix of Sn, the formation of $Li_{15}Si_4$ can be suppressed, leading to good cycling.
- Immiscible gap between Si and Sn, and low melting point of Sn (232 ^{0}C) appear to be challenges.
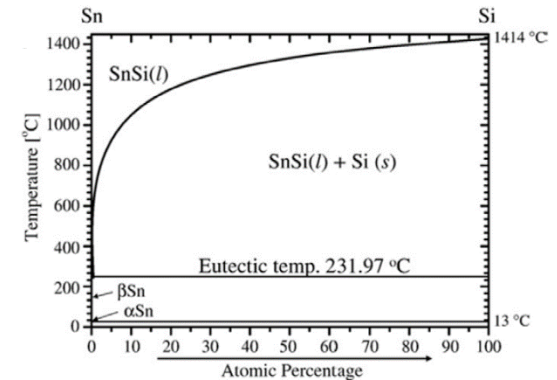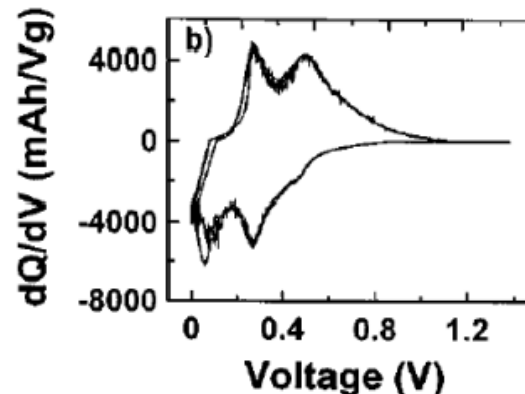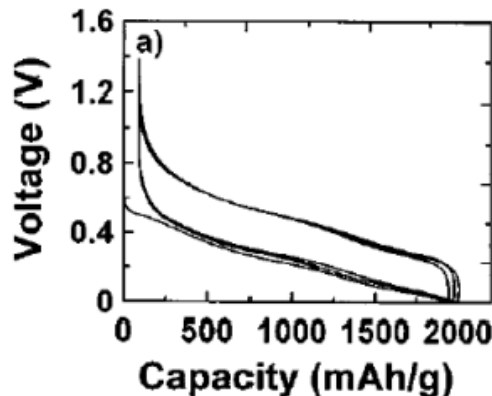
J. Electrochem. Soc. **150**(2) A149 (2003)

J. Phys. D: Appl. Phys. **47** (2014) 393001.

Amorphous $Si_{0.64}Sn_{0.36}$

- Amorphous $Si_{0.64}Sn_{0.36}$ thin film exhibits a high capacity (2000 mAh/g) and low irreversible capacity (100 mAh/g).

- Immiscible gap between Si and Sn, and low melting point of Sn (232 ^{0}C) appear to be challenges.
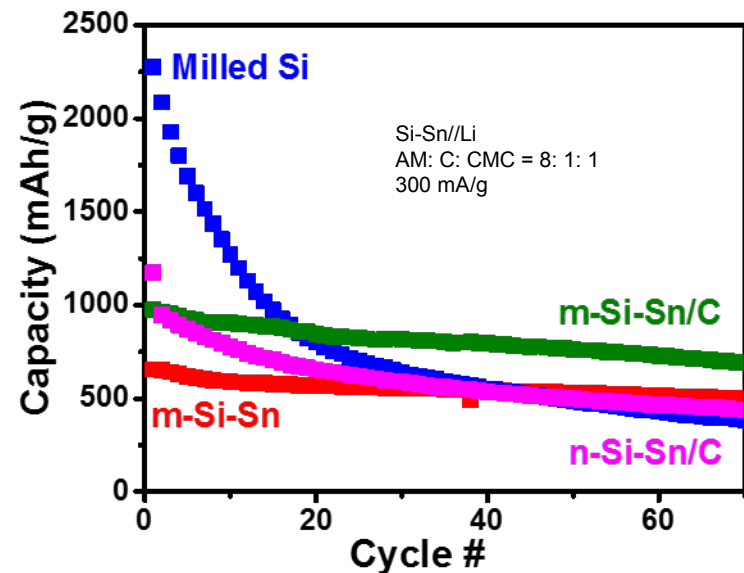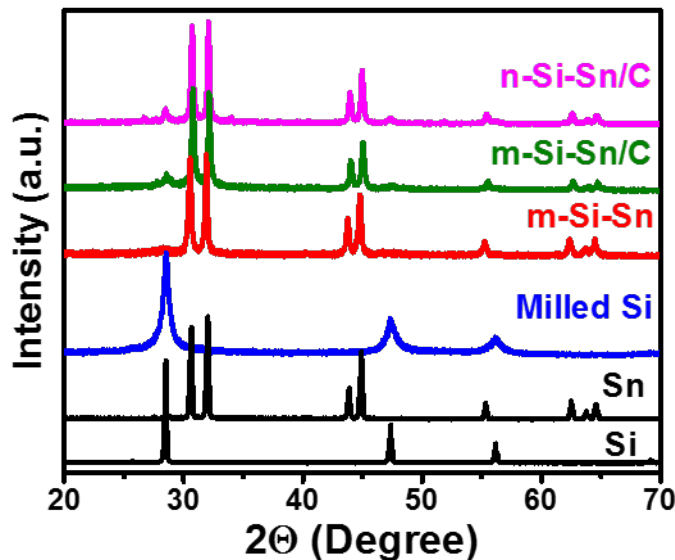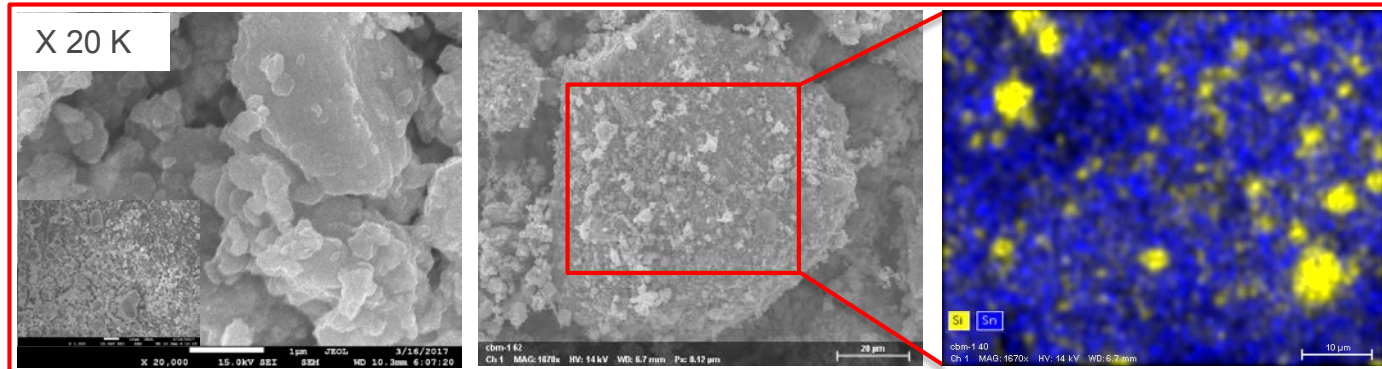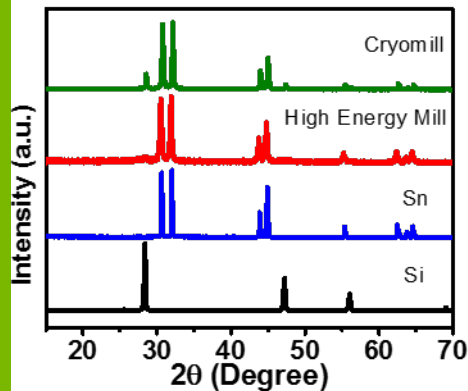

- Goal is to achieve homogeneous mixing of electrochemically active Si and Sn.
- High energy milling at room temperature tends to cause particle agglomeration although carbon tends to alleviate it.
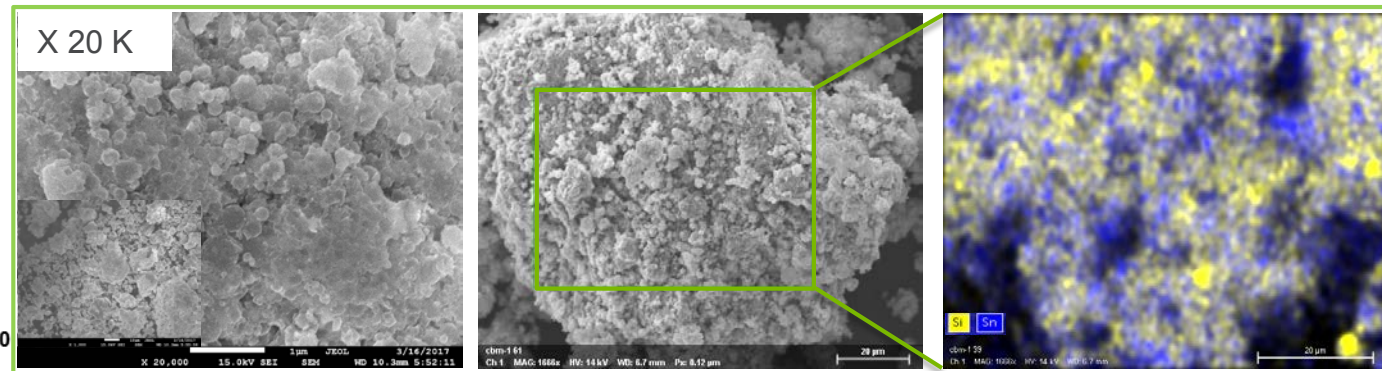
Amorphous $Si_{0.64}Sn_{0.36}$ by Cryomilling
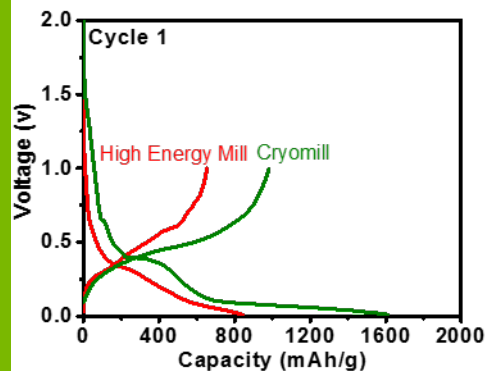
- Cryomill tailored for cryogenic grinding to cool a jar by liquid nitrogen during milling and offers the potential to break down particle size, achieve good mixing, and avoid Sn melting.
- Cryomill is less effective in decreasing Si crystallinity, but leads to much more homogeneous mixing between Si and Sn without use of carbon.

2. Functional Polymer Binders

2.1. Multi-grafting Block Copolymer

▪ Design principal

Design and synthesize a water-soluble polymer binder with well-defined architectures.

Systematical study on the architecture-property relationship on the polymer binder performance for silicon/graphite composite anode.

- Compare the multi-grafting chitosan-*g*-lithium acrylate with linear analogue, i.e., chitosan and physical mixing of chitosan and lithium acrylate.
- Study the length of the side chain on the multi-grafting polymer.
- Study the grafting density of the multi-grafting polymer.
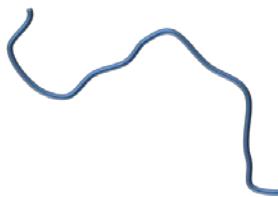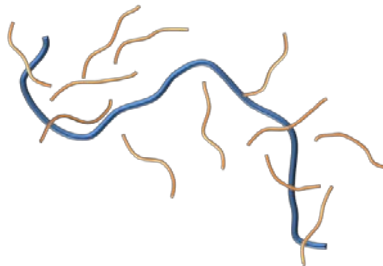
Chitosan   Chitosan-*m*-LiPAA   Chitosan-*g*-LiPAA

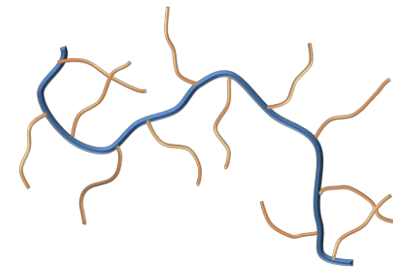# Synthesis & Characterization of Multi-Grafting Chitosan-g-LiPAA

Chitosan-*g*-LiPAA

Side chain length:
$DP_n = 1/2(63.55 + (120.59/2)) = 61.9$
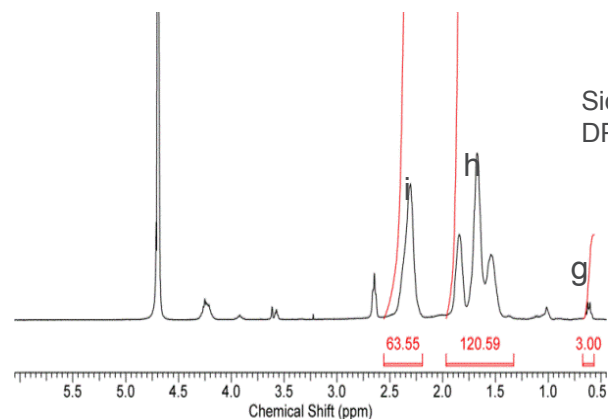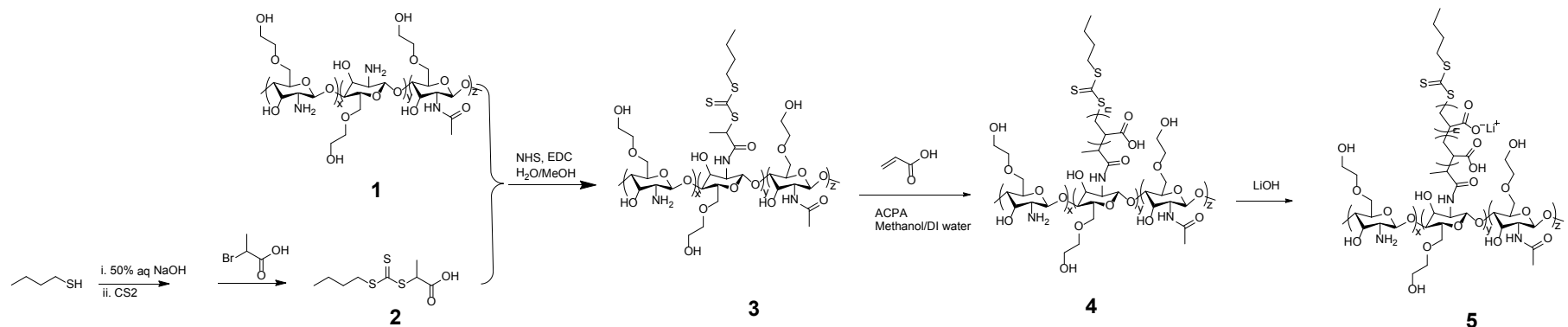
^{1}H NMR spectrum of compound **4** for **side chain length** calculation
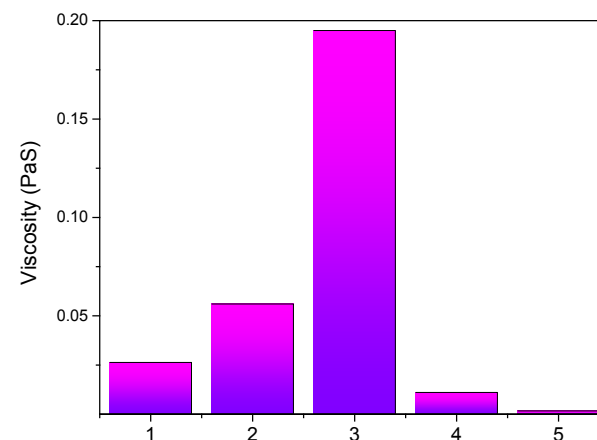
Measured Viscosity of different polymer-binder solutions with the same polymer content (1wt%): 1. Chitosan-*g*-LiPAA16, 2. Chitosan-*g*-LiPAA27, 3. Chitosan-*g*-LiPAA62, 4. Chitosan-*m*-LiPAA76, 5. Chitosan

Comparative Cycling Performance of PVDF, Chitosan, Chitosan-*m*-LiPAA, Chitosan-*g*-LiPAA
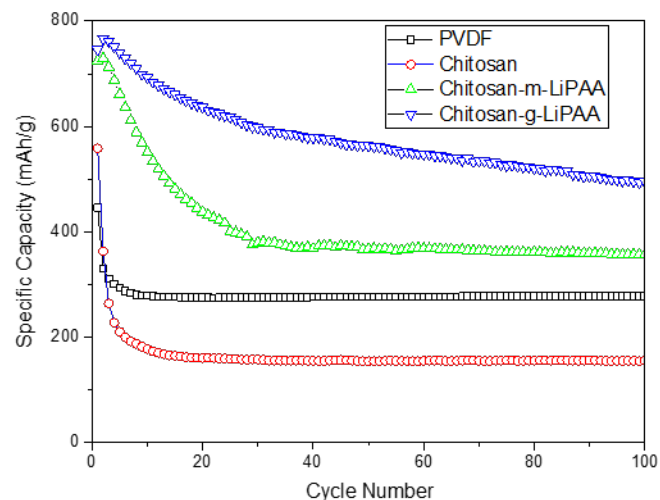
Comparative delithiation capacity
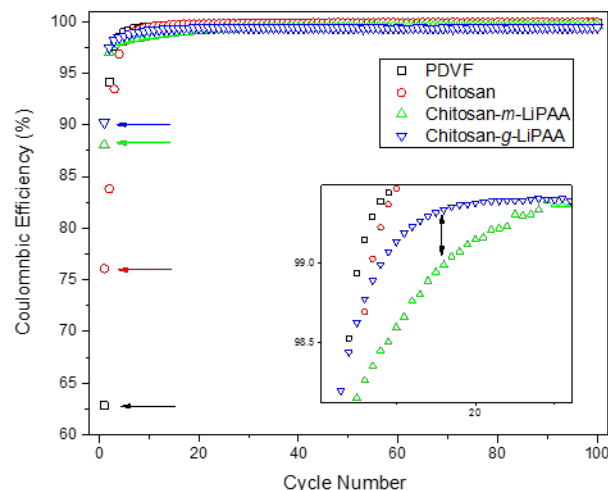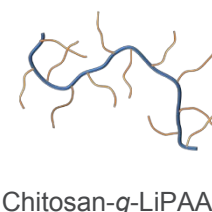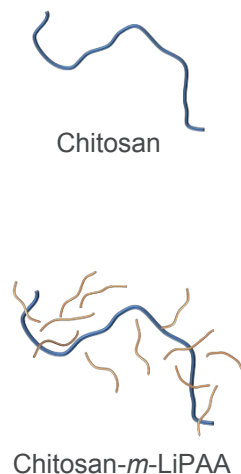
Comparative coulombic efficiency

Chitosan

Chitosan-*m*-LiPAA

Chitosan-*g*-LiPAA

Side chain length impact on performance of chitosan-*g*-LiPAA binder
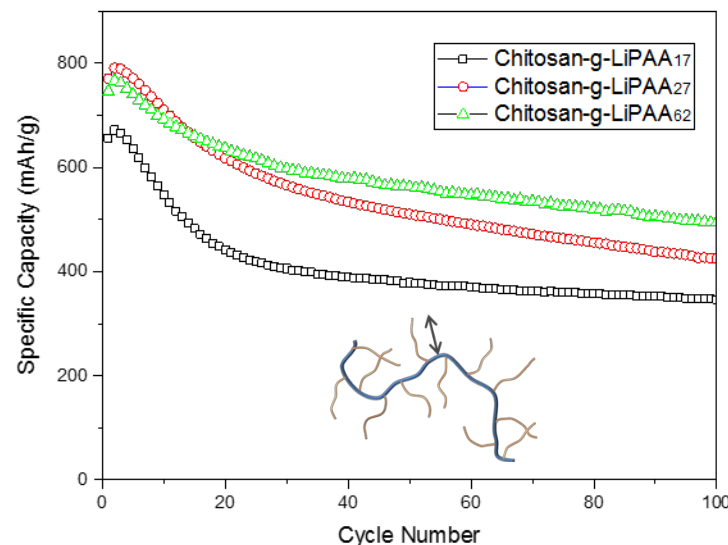
✓ Polymer architecture and side chain length played a significant role on the cell performance.

✓ Multi-grafting chitosan-*g*-LiPAA exhibited improved performance compared with its linear analogues (i.e. PVDF, chitosan, physical mixture of chitosan and LiPAA, and LiPAA).

2.2. Polysiloxane-Based Comb Polymers

- Polysiloxane (PS) structural similarity (Si-O-Si) to silica could be beneficial to the performance of Si.
- PS can be engineered towards certain desirable properties, such as flexibility, 3-D networking, strong adhesion and conductivity by introducing functional groups.
- A variety of functions can be introduced onto the PS architecture with adjustable ratios to afford binders with desirable properties and understand the Property ~ Property Relationship.

AGE Cross-linking **AMPEO₃** Flexibility **VTMS** Adhesion **PPy** Conductivity

A Cross-linking
B Flexibility
C Adhesion
D Conductivity

PMHS-1 PMHS-2 (uncrosslinked) PMHS-4 PMHS-5
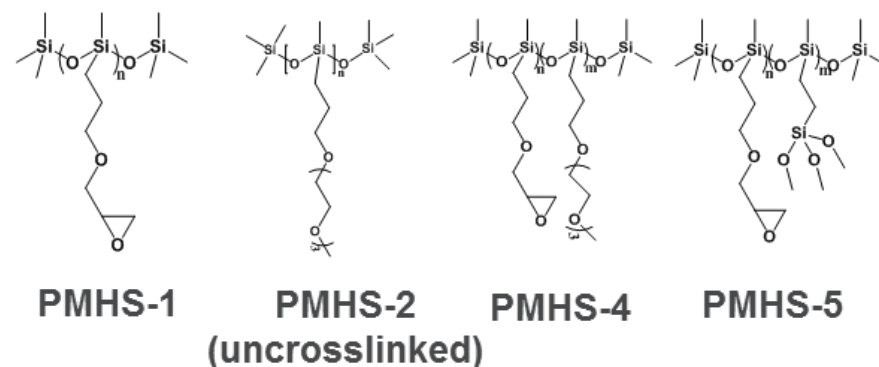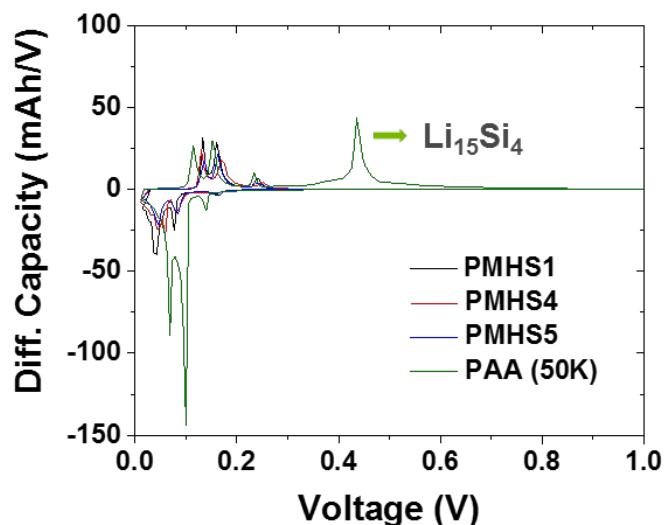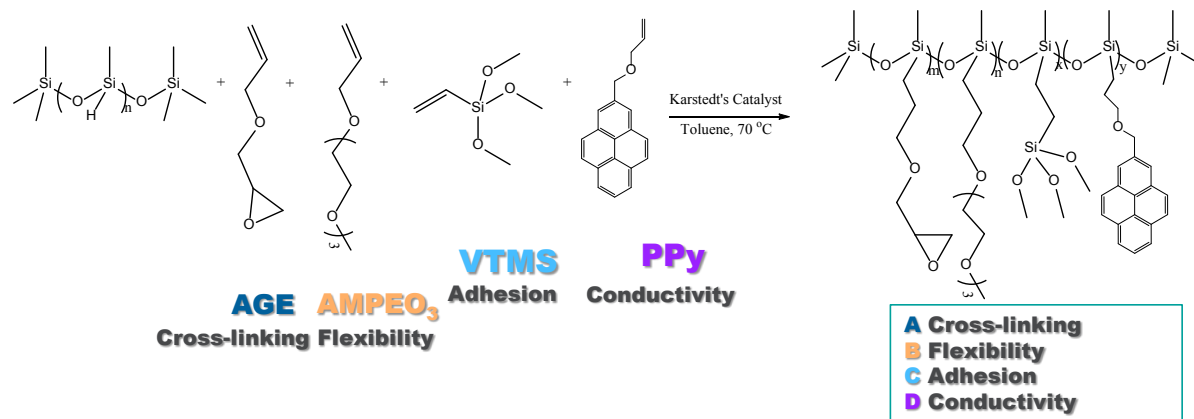
The characteristic $Li_{15}Si_4$ phase only shows up in PAA cells.
No such peak can be observed for PS binder cells, indicating the PS binders alter the reaction pathway of silicon particle during lithiation process.

2.3. Poly(carboxylic acid)-Based Binders

PVDF ⟹ PAA LiPAA

LiOH
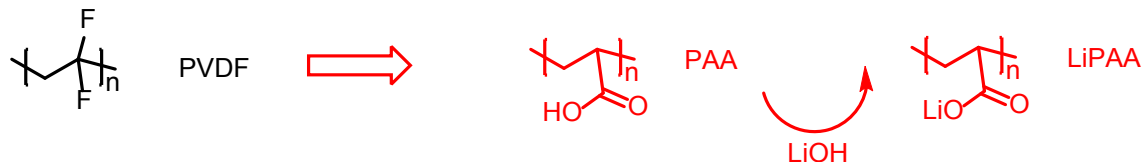
M_n (GPC): PAA3>PAA1>>PAA2>PAA4>>PAA5

Entry	Vendor	Mn	Mw	Mv	PDI
PAA-1	Aldrich	175.1 K	851.7 K	702.4 K	4.86
PAA-2	Aldrich	43.1 K	147.7 K	125.6 K	3.43
PAA-3	Aldrich	199.4 K	1151.8 K	937.8 K	5.78
PAA-4	Polysciences	29.1 K	90.6 K	78.3 K	3.11
PAA-5	Acros	3.6 K	6.8 K	6.2 K	1.89
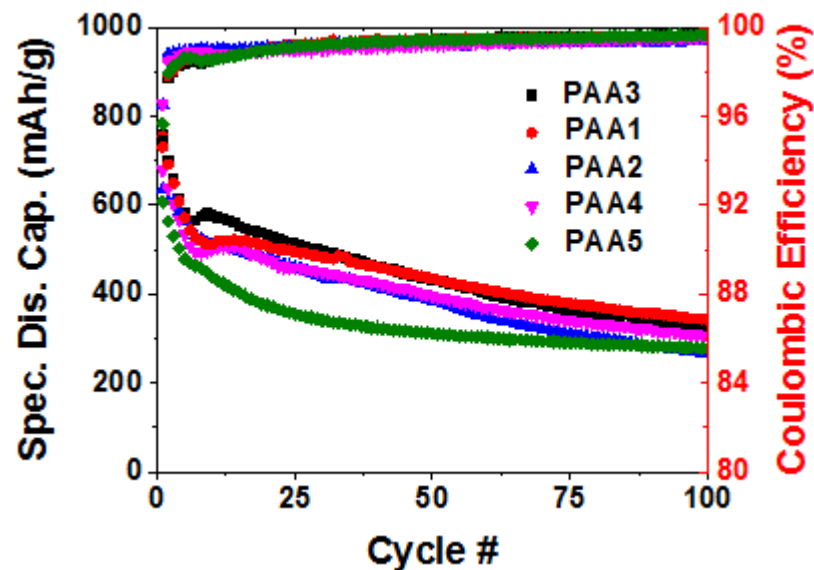
- The molecular weights indeed impacted the cycling performance.
- High molecular weight PAA binders showed improved performance in terms of initial capacity and capacity retention.
- Among PAA1 to PAA4, when the M_n is between 30 K to 200 K, the cycling performance is very close. Below a certain M_n, such as PAA5 (4 K), the performance becomes much worse.

2.4. Poly(carboxylic acid)-Based Conducting Binders

Electrode based on functional conductive PPy binder is fabricated at the similar composition, loading, and porosity to the LiPAA and PVDF electrode.
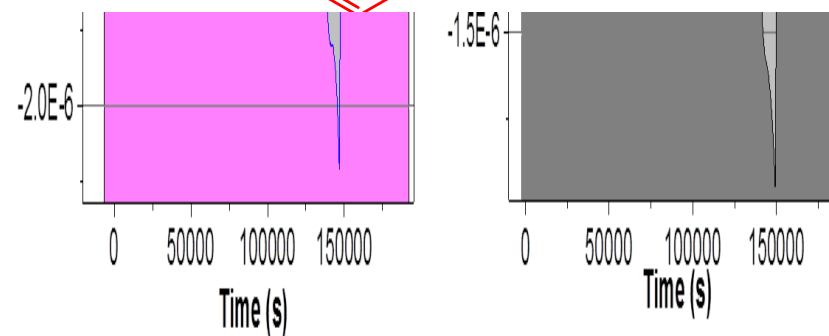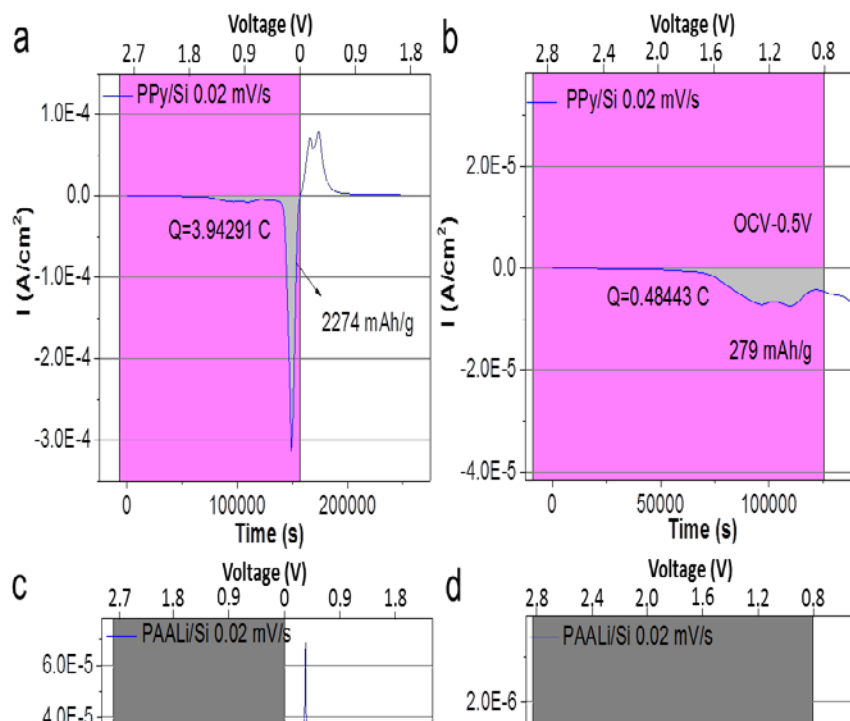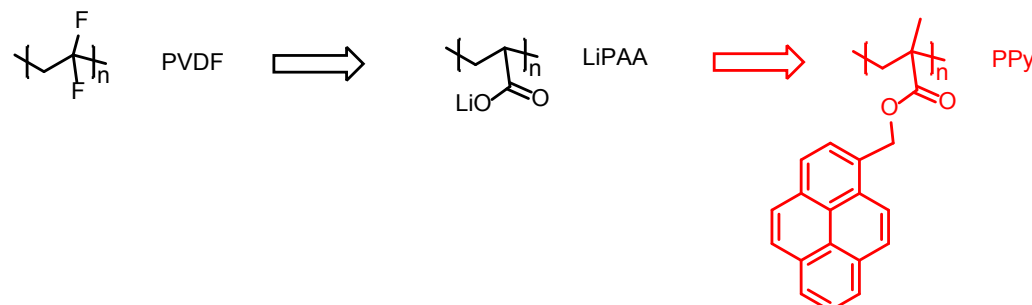
The CV reduction scan of Si/PPy (a, b) and Si/LiPAA (c, d) electrodes shows additional reduction wave/capacity from the PPy based electrodes.

The CV reduction scan of PPy (e) and LiPAA (f) thin film on Cu foil in the lithium-ion electrolyte with Li reference and counter electrode indicates additional reduction wave/capacity from the PPy polymer.

Pristine PPy binder based electrode, compared to LiPAA, has better Si nanoparticle dispersion on graphite, shows uniformed particle expansion when lithiated, and invoke less surface cracking after delithiation.

a PAALi Pristine 100,000×

b PAALi Pristine 5,000×

c PPy Pristine 100,000×

d PPy Pristine 5,000×

e PAALi lithiated 100,000×

f PAALi lithiated 5,000×

g PPy lithiated 100,000×

h PPy lithiated 5,000×

i PAALi delithiated 100,000×

j PAALi delithiated 5,000×

k PPy delithiated 100,000×

l PPy delithiated 5,000×
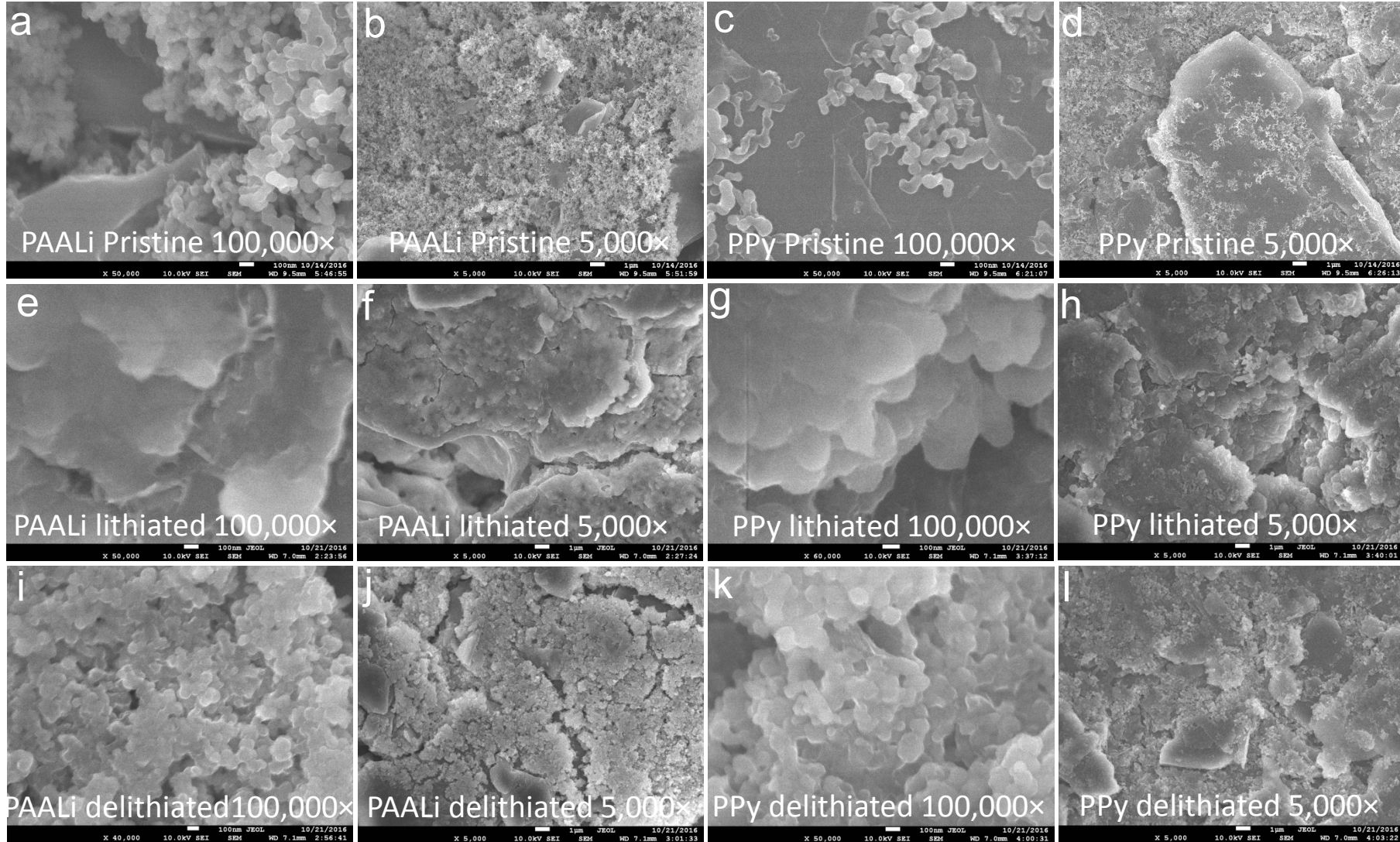
PPY Binder Cycling Performance and Post-Test Analysis
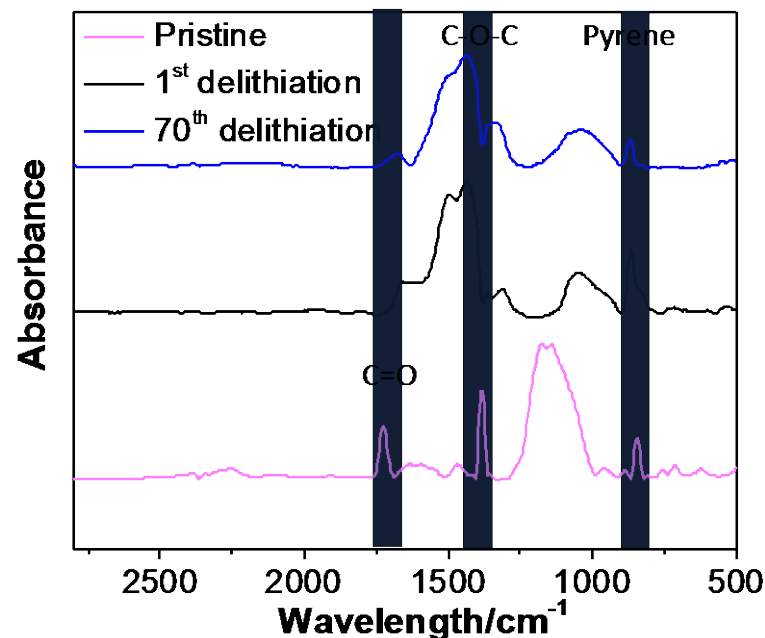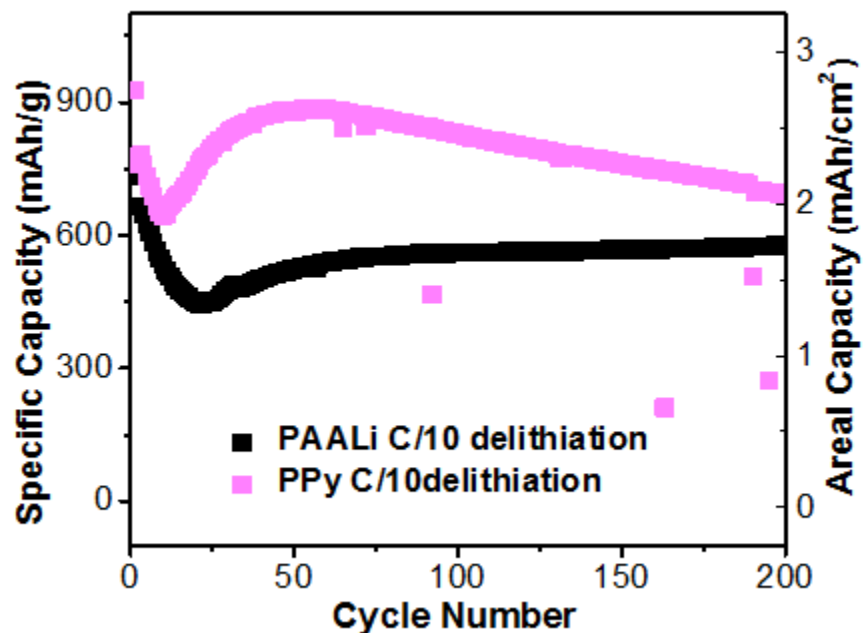
- ✓ PPy binder based electrode has higher initial cycling capacity compared to the LiPAA binder based electrode.

- ✓ The PPy binder is stable during electrode cycling test. The pristine electrode, the electrodes after 1st and 70th cycles show the existence of the pyrene functional groups based on FT-IR, while extensive SEI formation has masked the carbon oxygen signature vibrations as we previously reported.

3.1. Si Surface Modification Using MLD - Electrode Level

Silicon electrodes with different loading mass were used to study the effect of MLD alucone coating on the physical and electrochemical properties.

- TMA $(Al(CH_3)_3)$ and glycerol $(C_3H_5(OH)_3)$ were used as precursors to form aluminum glycerol (AlGL)16 coating.

- Step A: $R\text{-}OH^* + Al(CH_3)_3 \rightarrow R\text{-}O\text{-}Al(CH_3)_2^* + CH_4$

- Step B: $R\text{-}O\text{-}Al(CH_3)^* + C_3H_5(OH)_3 \rightarrow R\text{-}O\text{-}Al\text{-}OC_3H_5(OH)_2^* + CH_4$
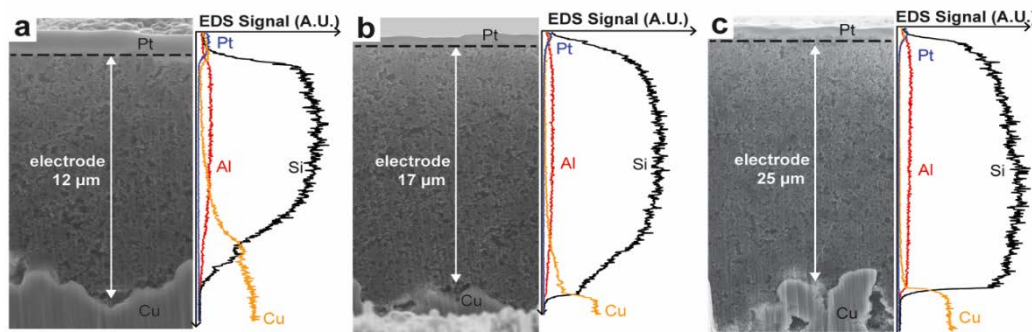
Cross-sectional SEM images of MLD coated electrodes with EDS line scanning for electrodes with different thickness and Si loading (a) 0.43 mg/cm^2, (b) 0.63 mg/cm^2 and (c) 0.79 mg/cm^2.
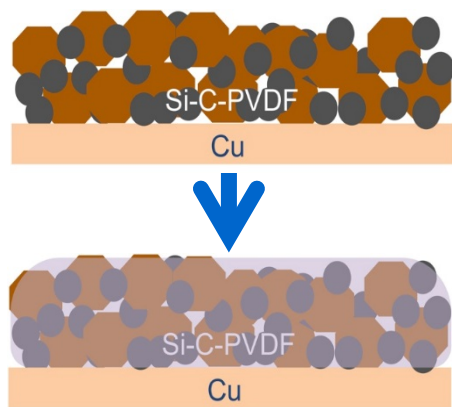
Si (60%)- CB(20%)-PVDF(20%)
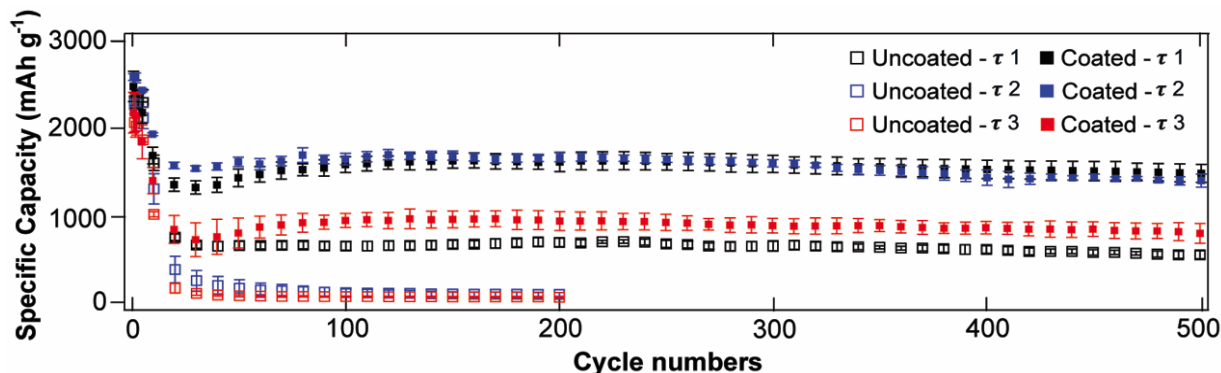
3. Si Surface Modification Using MLD – Particle Level
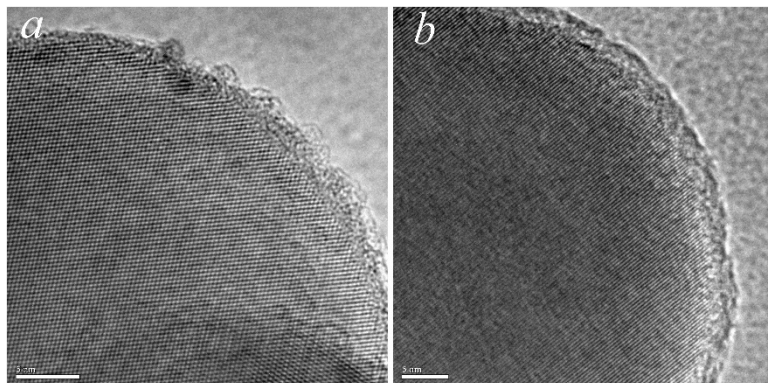
TEM images of Si particle #1 (Alfa Aesar)

(a) Uncoated Si particle

(b) MLD-coated Si particle
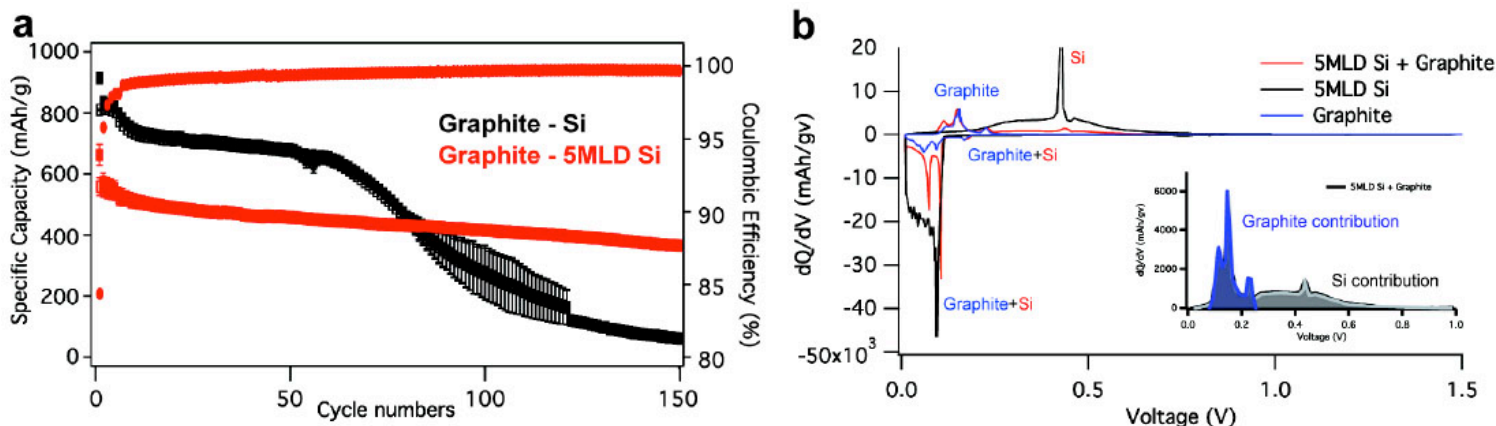
✓ Electrode composition: Graphite-Si-CB-PAA, 73 wt.%-15 wt.%-2 wt.%-10 wt.%. Cycling condition: 90mA/g between 10 mV and 1 V.

✓ Addition of 15 wt.% of Si #1 into the graphite based electrode results in the increase of specific capacity from 372 mAh/g to 918 mAh/g with improved Coulombic efficiency.

✓ Improved cycling performance was observed for the graphite-coated Si composite electrode (red) over the graphite-uncoated Si composite electrode (black).

✓ Capacity contribution was identified by the differential capacity (dQ/dV) profiles of the electrodes made with the graphite, the MLD-coated Si and the graphite-coated Si.

4. Si Surface Modification by SEI - Electrolyte/Additive
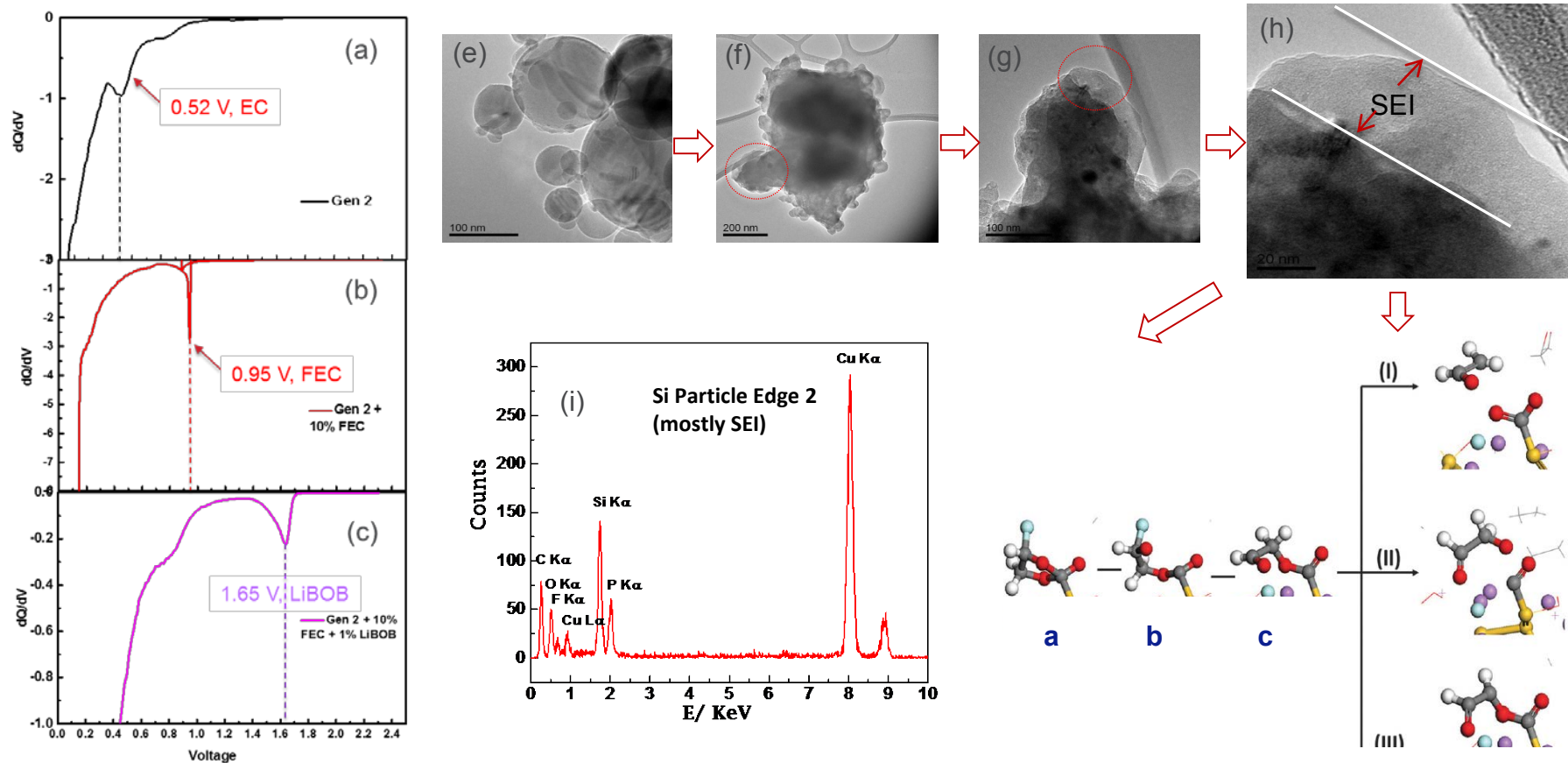
- ➤ Electrochemical reduction reaction of SOA electrolyte and the additives at different potentials (*a-c*).
- ➤ Electrochemically *in-situ* SEI formation on the Si particle surface stabilizing the interface (*e-h*).
- ➤ SEI formed via FEC reduction comprises both inorganic (LiF) and organic polymerization product (i).

Silazane-Based Compounds as Electrolyte Additives

Gen2+ 10% FEC+0.5% Additive
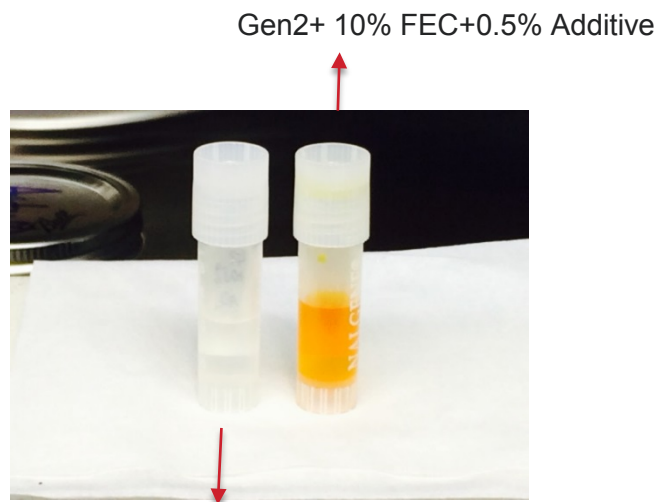
Gen2+ 5% Additive

Synergistic Effect

1.0 V, FEC

Gen 2 + 10% FEC

1.0 V, FEC

1.45, 1.55 V, HMDS & complex

Gen 2 + 10% FEC + 5% HMDS
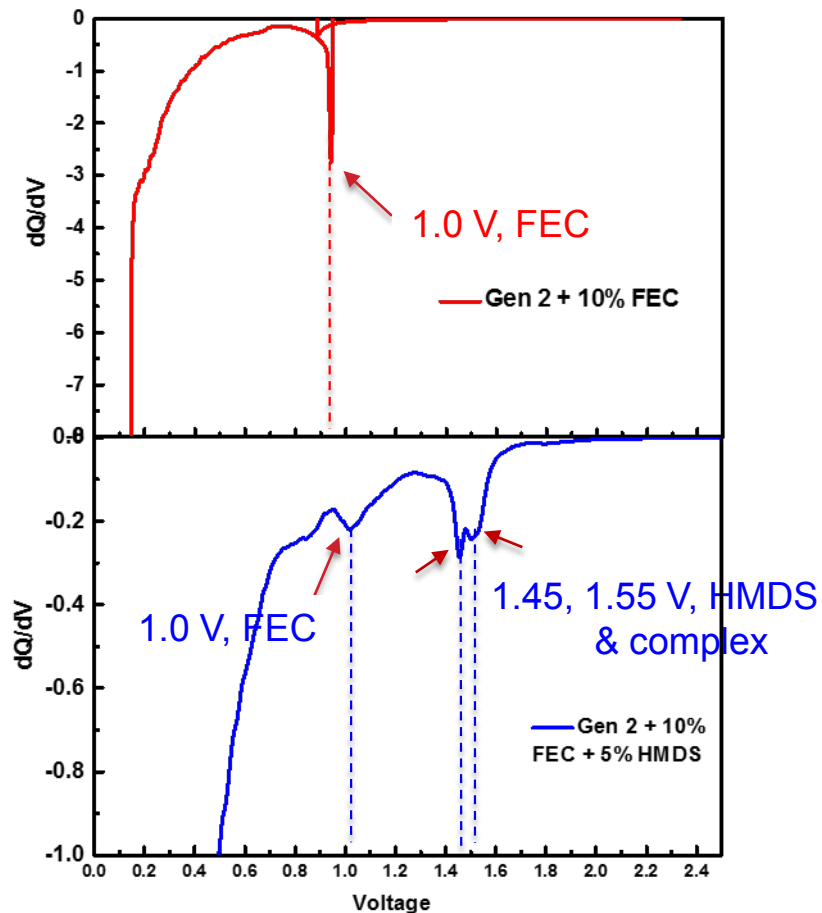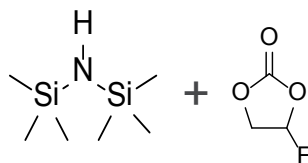
✓ Silazane compound does not interfere with the reduction of FEC.
✓ New SEI was formed with the dual additives and SEI formation.
✓ Extra reduction peak associated with Silazane additive is due to the strong hydrogen-bonding.

Interfacial Impedance Evolution with Cycling
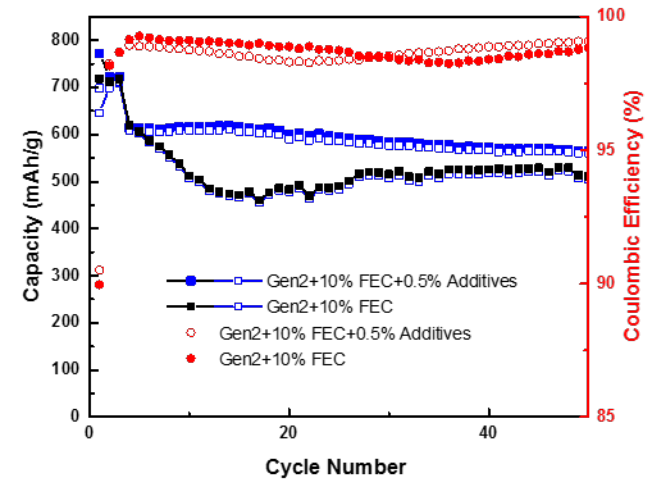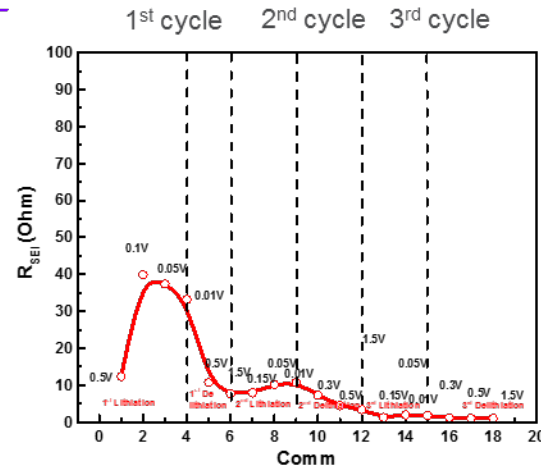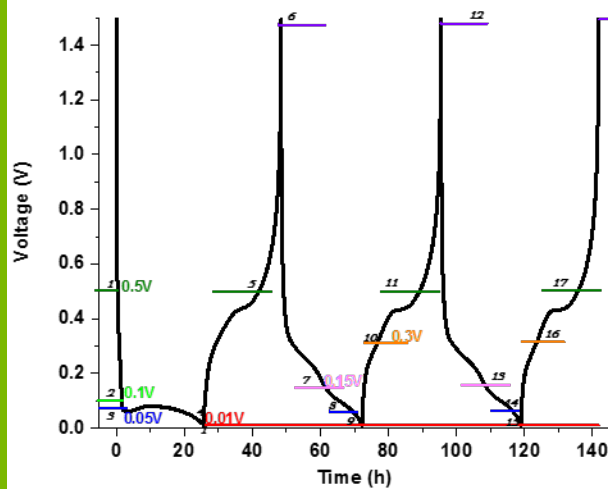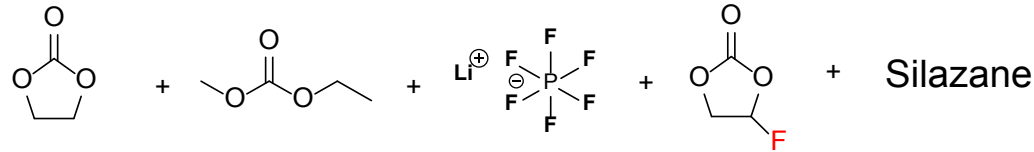
- ✓ SEI formation varies with electrolyte/additive and dependent on the lithiation stages or anode potential.
- ✓ Highly resistive and more-organic like SEI film formed during the initial lithiation process for Gen2 cell.
- ✓ Dense and more conductive SEI formed at the initial and subsequent cycles for both additive cells.
- ✓ Not only SEI thickness and morphology, the chemical composition of the SEI matters.
- ✓ FEC/Silazane synergistic effect was observed for the cycling performance.

5. Lithium Inventory to Counter Initial Capacity Loss and Subsequent Capacity Loss During Cycling

- Li_5FeO_4 (LFO) is proposed to help mitigate the first cycle capacity loss by providing an addition source of lithium when added to the cathode material.

- Optimize the synthesis and produced at least 10 batches of LFO pre-lithiation additive for the cathode.

- Li-inventory activity verified by electrochemistry.

  - > 700 mAhg$^{-1}_{LFO}$ first charge to cutoff of 4.4 V; 100 or

  10 mAg^{-1} current density with no capacity fall off.

Li/Fe = 5

Vacancy O^{2-} Li^+

14O
1 Fe
5 Li
2 vac.

Isolated $[FeO_4]^{5-}$ unit

Fe^{3+}

- Transferred the material synthesis to MERF personnel as reference for scale-up.
- No deleterious effects using LFO with NMC523 electrochemistry.
- No dissolution of LFO found.
- Low impedance confirmed with AC impedance and current interrupts.
- Scale-up lithium iron oxide is actively pursued at MERF and material has been scaled reproducibly at >100g to the 600°C intermediate.

Sandia National Laboratories

OAK RIDGE National Laboratory

NREL NATIONAL RENEWABLE ENERGY LABORATORY

BERKELEY LAB

Argonne NATIONAL LABORATORY
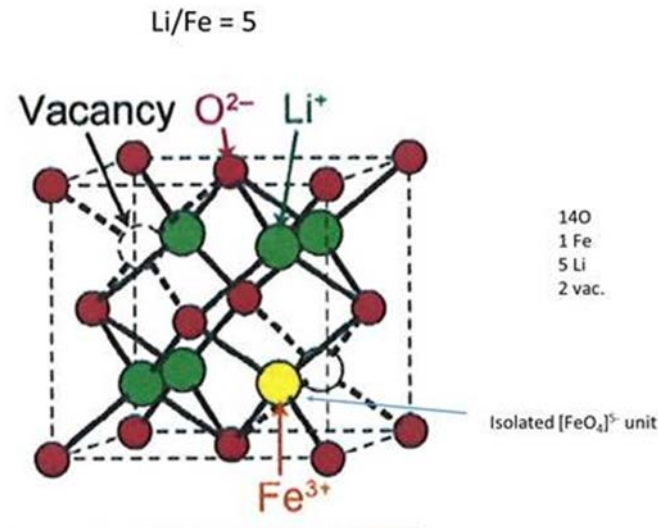
Li$_5$FeO$_4$ Li-Source Additive Electrochemistry
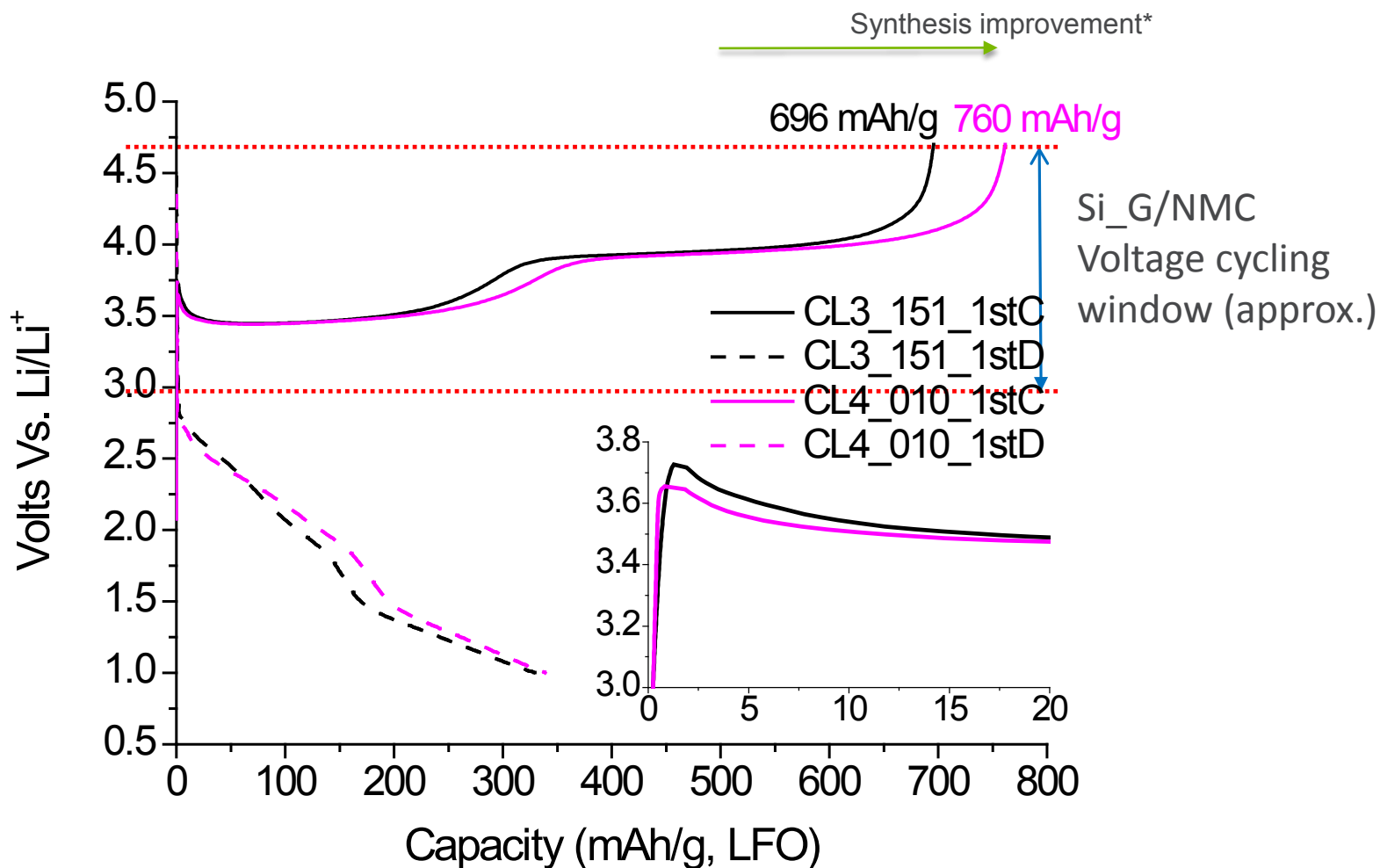
*   Li-source (~4.4 Li/Fe) for use to pre-lithiate Si (on first charge)

Employ An Iron Oxide Nanophase to Improve Reaction Kinetics & Thermodynamics

Synchron X-ray Diffraction

— 800°C, pure LFO
— 600°C, LFO + 20% α-LiFeO$_2$
— precursor, γ-Fe$_2$O$_3$, nanosize

· γ-Fe$_2$O$_3$ · α-LiFeO$_2$ · LFO

2θ (λ=1.5418 A)

LFO product
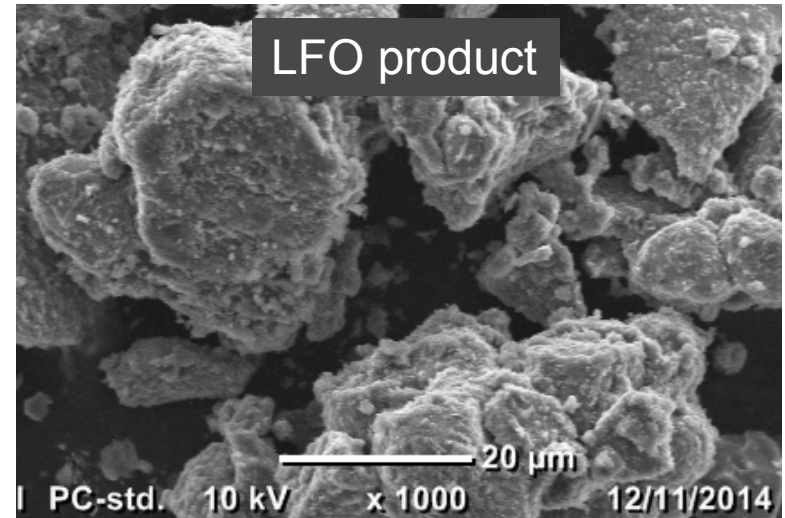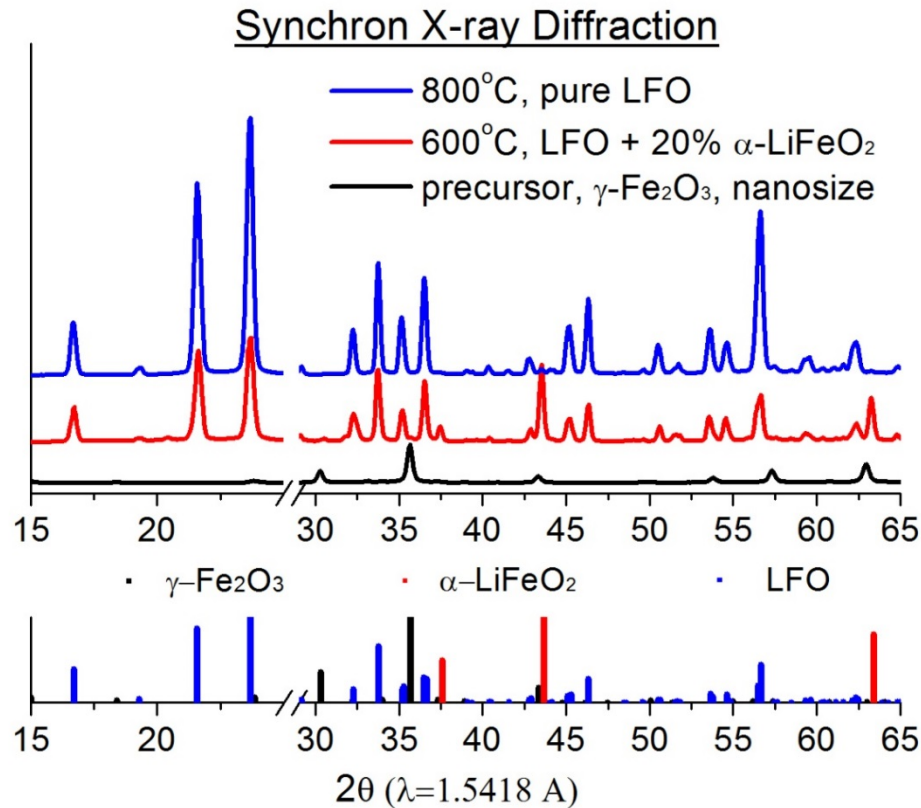
Precursor, <50 nm → LFO, ~ 20 μm

- The precursor was identified as γ-Fe$_2$O$_3$ (Fe$_3$O$_4$ with Fe defect)

- Nanoparticles of Fe$_2$O$_3$ help the formation of LFO.
- LFO pure phase was formed at 800°C, w/o intermittent grinding.
- At 800°C, sintering promoted by high Li content.

LFO/NCM 523 Cycling (4.5% LFO Li-Inventory Additive)

Li half cell

20% ICL
523 alone 10-11% ICL

LFO indicator

- sx539Charge
- sx539Discharge
- sx542Charge
- sx542Discharge

LFO indicator
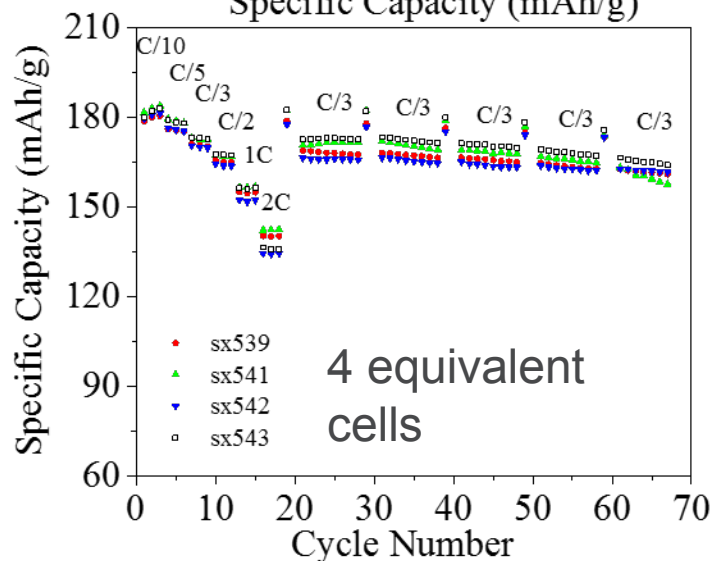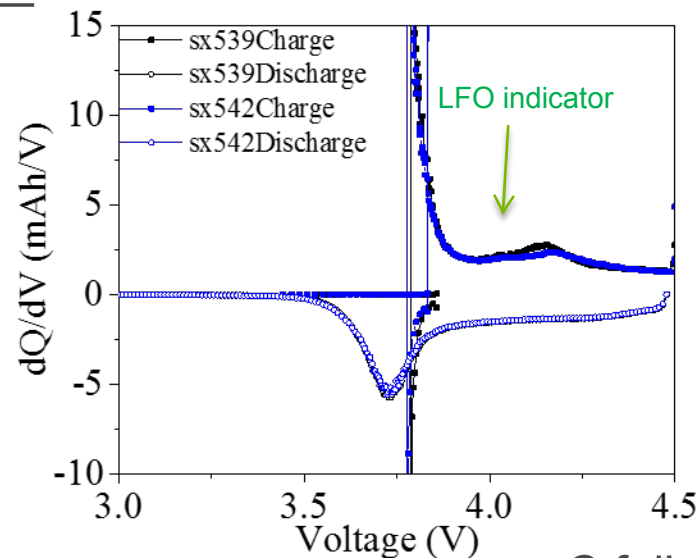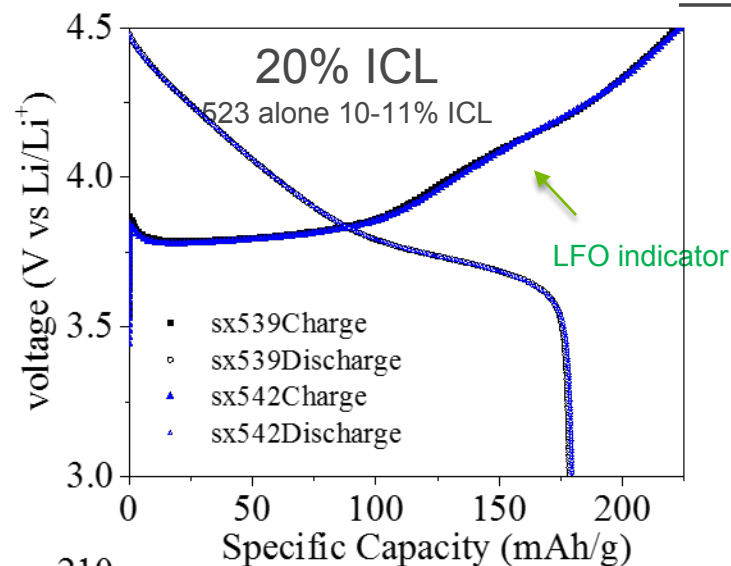
C full cell
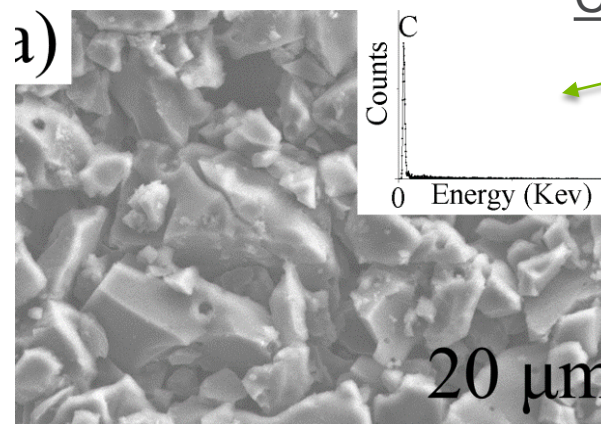
No Fe
in EDAX
spectrum
(no LFO
dissolution)

- sx539
- sx541
- sx542
- sx543

4 equivalent
cells

Dry room processed electrodes

REMAINING CHALLENGES AND BARRIERS

- Several key challenges remain that limit integration of silicon into graphitic negative electrodes, mostly related to the large crystallographic expansion of silicon (>300%) upon lithiation.
  - Particle cracking, particle isolation, and electrode delamination.
  - SEI stability issues, which affect cycling efficiency.

RESPONSES TO PREVIOUS YEAR REVIEWERS' COMMENTS

- We thank the reviewers for their comments, most of which were positive.
  - "outstanding effort to systematically assess advanced anode systems"
  - "preliminary work on program structure, material standards and protocol standards appears to be moving along well"
  - "a good use of resources/synergies of the national laboratories"
- One reviewer pointed out the importance of building in flexibility into this program, which we totally agree and have experienced.
  - "the resource structure may have to change over time with new understanding"
- We apologize that we were not more clear concerning our openness to industrial participation, but that all participation must be open to the whole community.
  - "collaboration is currently with internal contributors, and the reviewer was unclear if industrial partners are sought after or anticipated"

FUTURE WORK

Future Efforts Focused on Building and Expanding Early Materials Development Studies

- Continue the divergent/convergent approach to further advance the materials developments.

- Continue in-depth understanding of the Si electrode degradation mechanisms from the material perspective using sophisticated *in-situ* and *ex-situ* diagnosis in collaboration with diagnosis team and post-test facility.

- Establish general rules dictating the structure-property relationships for Si-based materials and electrodes.

- Verify the material candidates that showed promising results in a full cell format.

- Scale up new materials (Si-Sn alloy, binders, electrolyte/additive, lithium inventory additive) and MLD coated electrode for performance verification.

Any proposed future work is subject to change based on funding levels.

SUMMARY

✓ Collaborative multi-National Lab research was performed on the materials and technology development to understand the fundamental phenomena that control the performance of the Silicon composite electrodes.

✓ Amorphous $Si_{0.64}Sn_{0.36}$ thin film prepared by cryomilling exhibits a high capacity (2000 mAh/g) with low irreversible capacity (100 mAh/g). Cryomill is less effective in decreasing Si crystallinity, but leads to much more homogeneous mixing between Si and Sn without carbon.

✓ A collaborative binder working group (BWG) was formed within the program focusing on the study of binder-dependent electrode degradation mechanism.

✓ BWG research shed lights on the correlation between the polymer structure and the physical and electrochemical properties of the Si composite electrode, including nature of the polymer, molecular weight and its distribution, polymer architecture (linear, physical mixture, block-copolymer, cross-linked polymer, combed polymer *et al*.).

✓ Si anode surface modification was engineered via MLD technique on both electrode level and Si particle level and *in-situ* formation of passivation on Si surface via functional electrolyte/additive.

✓ Li_5FeO_4 (LFO) was verified as an effective lithium inventory to counter initial capacity loss of Si electrode. The synthesis of LFO was optimized and scaled up at MERF facility at ANL.

CONTRIBUTORS AND ACKNOWLEDGMENT

Research Facilities
- Post-Test Facility (PTF)
- Materials Engineering Research Facility (MERF)
- Cell Analysis, Modeling, and Prototyping (CAMP)
- Battery Manufacturing Facility (BMF)
- Battery Abuse Testing Laboratory (BATLab)

Contributors

- Daniel Abraham
- Eric Allcorn
- Seong Jin An
- Chunmei Ban
- Javier Bareno
- Ira Bloom
- Anthony Burrell
- Pengfei Cao
- Yang-Tse Cheng
- James Ciszewski
- Claus Daniel
- Dennis Dees
- Fulya Dogan Key
- Wesley Dose
- Zhijia Du
- Alison Dunlop
- Trevor Dzwiniel
- Kyle Fenton
- Kevin Gallagher
- Steve George

- James Gilbert
- Jinghua Guo
- Atetegeb Meazah Haregewoin
- Kevin Hays
- Bin Hu
- Andrew Jansen
- Christopher Johnson
- Kaushik Kalaga
- Baris Key
- Robert Kostecki
- Gregory Krumdick
- Jianlin Li
- Min Ling
- Gao Liu
- Wenquan Lu
- Jagjit Nanda
- Kaigi Nie
- Ganesan Nagasubramanian
- Christopher Orendorff
- Bryant Polzin
- Krzysztof Pupek

- Philip Ross
- Rose Ruther
- Niya Sa
- Tomonori Saito
- Yangping Sheng
- Seoung-Bum Son
- Xin Su
- Robert Tenent
- Lydia Terborg
- Wei Tong
- Stephen Trask
- Jack Vaughey
- Gabriel Veith
- David Wood
- Koffi Pierre Claver Yao
- Liang Zhang
- Linghong Zhang
- Lu Zhang
- Shuo Zhang
- Zhengcheng Zhang
- Tianyue Zheng

Sandia National Laboratories

OAK RIDGE National Laboratory

NREL NATIONAL RENEWABLE ENERGY LABORATORY

BERKELEY LAB

Argonne NATIONAL LABORATORY

PUBLICATIONS/PRESENTATIONS

- S. Zhang, M. He, C.-C. Su, Z. Zhang*. Advanced Electrolyte/Additive for Lithium-Ion Batteries with Silicon Anode. *Current Opinion in Chemical Engineering*, *13*, **2016**, 24-35. DOI: 10.1016/j.coche.2016.08.003
- C. Ban*, S. M. George. Molecular Layer Deposition for Surface Modification in Li-ion Batteries. *Advanced Material Interface*, 2016, 1600762. DOI: 10.1002/admi.201600762
- K. E. Hurst, J. M. Luther, C. Ban, S. T. Christensen. "Nanomaterials for Energy Applications" In Mansfield, E.; Kaiser, D. L.; Fujita, D.; Van de Voorde, M. (Ed). Wiley **2016**
- D. M. Piper, Y. Lee, S-B. Son, T. Evans, F. Lin, D. Nordlund, X. Xiao, S. M. George, S.H. Lee, C. Ban*. Cross-linked Aluminum Dioxybenxene Coating for Stabilization of Silicon Electrodes. *Nano Energy, 22*, **2016**, 202-210. DOI: 10.1016/j.nanoen.2016.02.021.
- M. Ling, M. Liu, T. Zheng, T. Zhang, G. Liu. Investigating the Doping Mechanism of Pyrene Based Methacrylate Functional Conductive Binder in Silicon Anodes for Lithium-Ion Batteries. *Journal of The Electrochemical Society*, *164* (4), 2017, A545-A548.
- J. Xu, M. Ling, L. Terborg, R. Kostecki, G. Liu, W. Tong. Facile Synthesis and Electrochemistry of Si-Sn-C Nanocomposites for High-Energy Li-Ion Batteries. *Journal of The Electrochemical Society*, submitted.
- L. Terborg, M. Ling, K. Nie, A. Dahi, C. Wu, J. Guo, P.N. Ross, G. Liu and R. Kostecki. The Effect of Polymer Binder on Electrochemical Performance of Si/C Anodes. *PRiME 2016*, Oct. 2-7, 2016, Honolulu, Hawaii, USA.
- C. Ban. Structural Evolution of Lithium-ion Electrodes During Battery Cycling. *51st American Chemical Society's Midwest Regional Meeting (ACS-MWRM)*, Manhattan, KS, 2016.
- C. Ban. Surface Modification for Nanoscale Silicon Electrode Materials. *Department Seminar*, University of Maryland, 2016.
- C. Ban. Development of Silicon Anode for High-Energy Li-ion Batteries. *11th U.S.-China Electric Vehicle and Battery Technology Meeting*, Denver, Colorado, 2016.
- C. Ban. Surface Modification for Silicon-Based Alloy Materials. *Department Seminar*, University of Kentucky, 2016.
- C. Ban, C. Jiang. Examining Electrical Properties of Solid Electrolyte Interface on Silicon Electrodes. *PRiME 2016*, Oct. 2-7, 2016, Honolulu, Hawaii, USA.
- C. Ban. Surface Modification of Silicon Anodes for Durable and High-Energy Lithium-Ion Batteries. *18th International Meeting on Lithium Batteries 2016*. Jun. 19-24, 2016, Chicago, Illinois, USA.